# Cluster Identification and Properties of Outdoor Wideband MIMO Channel

Weihui Dong[†], Jianhua Zhang[†], *Member, IEEE*, Xinyin Gao[†], Ping Zhang[†], and Yufei Wu[‡]
[†]Key Laboratory of Universal Wireless Communication (Beijing University of Posts and Telecommunications), Ministry of Education
[‡]Motorola Ltd., Illinois 60196, America

***Abstract*—In this paper, the statistical analysis of cluster is presented based on the outdoor wideband multiple-input multiple-output (MIMO) channel measurements to facilitate IMT-Advanced system design. Clusters are found in multi-dimensional space, i.e., on the azimuth of arrival-azimuth of departure-elevation of departure-delay domain. We identify clusters with an automatic cluster identification algorithm and a new method is developed to improve the algorithm in terms of convergence rate and accuracy, which can also be used in calculating the angular spread (AS) to avoid the ambiguity caused by the origin of the coordinate system. All cluster parameters are described by a set of probability density functions (pdfs) derived from the measured data. The cluster numbers are well fitted with Poisson distribution plus a minimum number of clusters, and both the delay spread and angular spread exhibit the Lognormal distribution. It is concluded that the elevation angle should not be neglected when terminals are rounded by rich scatterers in outdoor scenario. We also find that clusters with smaller delays have in general a higher cross-polarization discrimination (XPD) than that with larger delays.**

***Index Terms*—Clusters, multiple-input multiple-output (MIMO), angular spread (AS), cross-polarization discrimination (XPD)**

## I. Introduction

BEYOND 3G (B3G) system has been named officially as 'IMT-Advanced' by International Telecommunication Union-Radio communications (ITU-R) in Oct. 2005 [1]. As for IMT-Advanced system, the RF bandwidth and carrier frequency will be up to 100MHz and 5GHz. The high frequency and wide bandwidth, together with deployment of multiple-input multiple-output (MIMO) system, are suitable for the hotspot application to provide high data-rate (maximal 1Gbps) transmission.

Recently a promising approach to model the MIMO channel involves the cluster concept [2]-[3]. Cluster is defined as a group of multipath components (MPCs) with similar parameters, e.g., angle of arrival (AOA), angle of departure (AOD), and delay in [2], [4] and [5]. Clustering can have a significant impact on channel capacity. Unclustered models tend to overestimate the capacity if the MPCs are indeed clustered [6].

Previous results based on the single-input multiple-output (SIMO) channels deploy visual inspection to identify clusters mostly on the AOA azimuth-delay domain in [2], [4] and [7]. However, it becomes cumbersome for our double-directional channel data, especially when we define the cluster in the multi-dimensional space, i.e., on the azimuth of arrival-azimuth of departure-elevation of departure-delay domain. Elevation angle is important when terminals are located in multipath rich environments, but only few studies on cluster are available for it. In this paper, we adopt an automatic cluster identification algorithm introduced in [8]. We develop a method to improve the algorithm in terms of convergence rate and accuracy, which can also be used in calculating the angular spread (AS) to avoid the ambiguity caused by the origin of the coordinate system. Up to now, most papers, e.g. [4] and [9], use the Fleury definition [10] and circular angle spread (CAS) [11] to calculate the AS. Fleury definition can only be used for small angular spread and CAS can't solve the ambiguity in fact.

Cross-polarization discrimination (XPD) is an important parameter to influence the gain of cross-polarized channels. In a recent study [12], the elevation spectrum and XPD is well modeled but cluster concept is not involved. Hence, besides the typical intra-cluster parameters, e.g., delay and angular spread, it is also necessary to investigate the cluster XPD and power properties versus delay.

## II. Measurement Setup And Environment

### A. Measurement Setup

(a) (b)

Fig. 1. Antenna arrays at 5.25 GHz: (a) 2x9 ODA. (b) 7+1 UCA.

The wideband MIMO measurements were performed with 100MHz bandwidth at 5.25GHz frequency using the Elektrobit Propsound [13] on the campus of Beijing University of Posts and Telecommunications (BUPT), China. Propsound is based on the principle of time division multiplexing. A measurement

The research is funded by National 863 Project: Wideband MIMO channel modeling and simulation in the next generation network (No. 2006AA01Z258), the 111 project (No. B07005) and Motorola Ltd.


(a) (b)

Fig. 2. Measurement scenario. (a) Top view of measurement route around the playground. (b) Picture of the playground enclosed by a grid fence made of steel.

snapshot refers to the time interval that all subchannels between transmitter (Tx) and receiver (Rx) antennas are sounded once. Propsound operates in burst-mode, i.e., there is a break after four measuring snapshots to allow real-time data transfer to the control laptop computer. These four snapshots are guaranteed within the coherence time of the channel to allow the channel parameter estimator to extract the channel parameters correctly.

As Fig. 1(a) shows, Tx consists of 50 dual-polarized patch elements while a subarray of 18 elements on a cylinder is used during the measurement. The polarization direction of the elements is $\pm 45^{\circ}$ slanted to vertical axes. Fig. 1(b) shows the vertically polarized uniform circular array (UCA) at Rx with 7+1 monopoles spaced by half the wavelength. It supports full azimuth direction probing but not the elevation. Hence, this pair of antennas can explore the channel properties of vertically polarized to vertically polarized (VP-VP) component and horizontally polarized to vertically polarized (HP-VP) component.

### B. Measurement Environment

The measurements were carried out on the playground of BUPT, as shown in Fig. 2. The playground was surrounded by a grid fence made of steel that might diffract propagating radio. During the measurements, Tx was mounted on the top of a car while moving around the playground with the speed of nearly 20km/h. Rx was mounted on a trolley fixed in the near centre of the playground. Measurements were conducted during day time when lots of people were playing basketball. During the measurement campaign, both Tx and Rx are positioned at the height of roughly 2m above the ground.

## III. Channel Estimator And Cluster Identification

### A. Channel Estimator

In our data post-processing, we choose SAGE algorithm [14] to extract the channel parameters which is particularly well suited for MIMO channel investigations. SAGE is based on the maximum likelihood (ML) method, which is categorized as the optimal technique, and allows joint estimation of delay, AOA, AOD, polarization matrix and Doppler shift.

Every four snapshots of measurement data are fed to SAGE and generate one set of channel parameters. In order to extract all the important paths that can correctly characterize the clustered scenario, an upper bound of multipath number is set to 50 and a cutoff threshold of 18dB below the strongest path is applied. In total, 141 sets of channel parameters are extracted.

Fig. 3 shows the estimated MPCs in one set on azimuth of arrival-azimuth of departure-elevation of departure-delay domain as well as their powers. It is noticeable that MPCs appear in several clusters by visual inspection. Therefore, next step is to identify the clusters accurately.

### B. Cluster Identification

We have choosen “multipath component distance” (MCD) metric based the automatic cluster identification algorithm [8]. The key feature of MCD, which was firstly introduced in [15], is that it normalizes each dimensional data of different units and gives different weights to different dimensions. We have considered both the delay and angular domain equally important, i.e., they have same weight.

However, some problems are found when calculating the cluster centroids and global centroid in KPowerMeans clustering algorithm and Caliñski-Harabasz index, respectively, discussed in [8]. Since they have the same problem, we take calculating the cluster centroids for example.

We consider a set of channel parameters with a number of L MPCs, where every single MPC is represented by its power $P_l$ [1], and a parameter vector $\mathbf{X}_l$ given by

$$\mathbf{X}_l = [\tau_l, \varphi_{AOA,l}, \varphi_{AOD,l}, \theta_{AOD,l}], \quad l = 1, 2, ..., L \tag{1}$$

where $\tau_l$, $\varphi_{AOA}$, $\varphi_{AOD}$, and $\theta_{AOD}$ are the excess delay, AOA azimuth, AOD azimuth and AOD elevation of the $l$th MPC, respectively. The $k$th cluster centroid $\mathbf{C}_k$ is calculated in [8] as

$$\mathbf{C}_k = \frac{\sum_{j \in \mathbb{C}_k} \mathbf{X}_j \cdot P_j}{\sum_{j \in \mathbb{C}_k} P_j} \tag{2}$$

where $\mathbb{C}_k$ denotes the MPC indices belonging to the $k$th cluster. Hence, each dimension value of $\mathbf{C}_k$ is the power weighted average of the corresponding dimensional data of MPCs within the cluster. When calculating the AOA azimuth or AOD azimuth of cluster centroid, attention should be paid on the ambiguity by the origin of the coordinate system. Hence, a new method is proposed as follows:

Let $\mathbb{C}_k$ be divided into two groups $\mathbb{C}_{k1}$ and $\mathbb{C}_{k2}$, classified by $\varphi_{j \in \mathbb{C}_{k1}} \geq 0$ *and* $\varphi_{j \in \mathbb{C}_{k2}} < 0$, where $\varphi_j$ is the AOA azimuth or AOD azimuth of the $j$th MPC. The corresponding dimensional

[1] In this paper, unless otherwise stated, the MPC power is the sum power of its VP-VP component and HP-VP component.

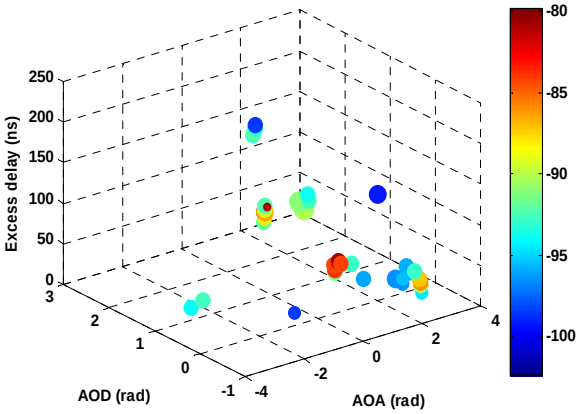


Fig. 3. The measured MPCs extracted by SAGE. The size of the balls is proportional to the AOD elevation. Colors represent the powers in dB.

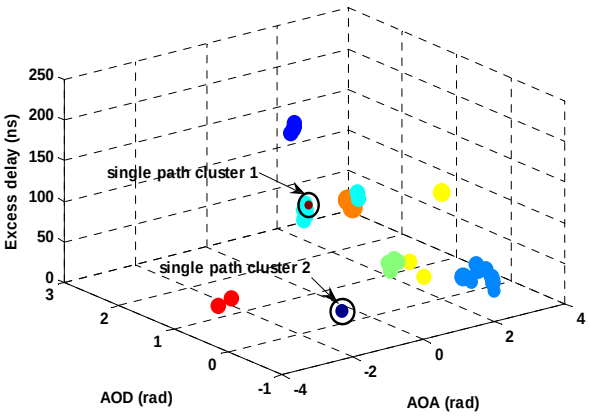


Fig. 4. Results after applying the automatic cluster identification algorithm. The size of the balls is proportional to the AOD elevation. 9 clusters are identified.

value of $\mathbf{C}_k$ is given by

$$\mu_\varphi = \frac{\sum_{j\in\mathbb{C}_k}\varphi_j\cdot P_j}{\sum_{j\in\mathbb{C}_k}P_j} = \frac{\sum_{j\in\mathbb{C}_{k1}}\varphi_j\cdot P_j + \sum_{j\in\mathbb{C}_{k2}}\varphi_j\cdot P_j}{\sum_{j\in\mathbb{C}_k}P_j} = \frac{\sum_{j\in\mathbb{C}_{k1}}P_j}{\sum_{j\in\mathbb{C}_k}P_j}\cdot\frac{\sum_{j\in\mathbb{C}_{k1}}\varphi_j\cdot P_j}{\sum_{j\in\mathbb{C}_{k1}}\varphi_j} + \frac{\sum_{j\in\mathbb{C}_{k2}}P_j}{\sum_{j\in\mathbb{C}_k}P_j}\cdot\frac{\sum_{j\in\mathbb{C}_{k2}}\varphi_j\cdot P_j}{\sum_{j\in\mathbb{C}_{k2}}P_j}. \quad (3)$$

Then we denote

$$\mu_{\varphi1} = \frac{\sum_{j\in\mathbb{C}_{k1}}\varphi_j\cdot P_j}{\sum_{j\in\mathbb{C}_{k1}}P_j}, \quad \mu_{\varphi2} = \frac{\sum_{j\in\mathbb{C}_{k2}}\varphi_j\cdot P_j}{\sum_{j\in\mathbb{C}_{k2}}P_j}. \quad (4)$$

Hence, $\mu_{\varphi1}$ and $\mu_{\varphi2}$ are the average values of nonnegative and negative angles, respectively. The ambiguity will appear by the origin of the coordinate system when $\mu_{\varphi1}-\mu_{\varphi2}>\pi$. So we define

$$\mu_{\varphi2}' = \begin{cases}\mu_{\varphi2}+2\pi & \mu_{\varphi1}-\mu_{\varphi2}>\pi\\ \mu_{\varphi2} & else\end{cases}. \quad (5)$$

Then $\mu_\varphi$ is changed to

$$\mu_\varphi = \frac{\sum_{j\in\mathbb{C}_{k1}}P_j}{\sum_{j\in\mathbb{C}_k}P_j}\cdot\mu_{\varphi1} + \frac{\sum_{j\in\mathbb{C}_{k2}}P_j}{\sum_{j\in\mathbb{C}_k}P_j}\cdot\mu_{\varphi2}'. \quad (6)$$

Since $\mu_\varphi$ may be beyond the range of $(-\pi,\pi]$, the final power weighted average of $\varphi$ is obtained as

$$\bar{\mu}_\varphi = \begin{cases}\mu_\varphi & \mu_\varphi\le\pi\\ \mu_\varphi-2\pi & else\end{cases}. \quad (7)$$

Fig. 4 shows the result after applying the automatic cluster identification algorithm. In this set (the same set in Fig. 3), 9 clusters are identified and 2 clusters denoted by circle consist of only one path each. The single path cluster 1 is not merged to the adjacent cluster because of the big difference of AOD elevations. It can be seen that the resulting partition realizes well trade-off between cluster compactness and separation.

## IV. Results

The automatic cluster identification algorithm is applied to all the sets of channel parameters and 1870 clusters are identified out of which 529 clusters are observed to be single path clusters. Single path clusters are not considered in the analysis of delay spread, angular spread and cluster numbers. There are so many single path clusters mainly because of the high dimensional cluster identification. Two parameter classes are given to describe the cluster properties: inter-cluster and intra-cluster parameters which characterize the cluster and MPC, respectively.

### A. Inter-cluster Properties

The distribution of the number of clusters $M$ in each set is plotted in Fig. 5. As to the COST 273 model [16], we model the probability density function (pdf) of $M$ as $N_{C\min}+X$, where $N_{C\min}$ is the minimum number of clusters and $X$ is a random variable with Poisson distribution given by

$$P(X=k) = \frac{\lambda^k}{k!}e^{-\lambda}, \qquad k=0,1,2,...14. \quad (8)$$

Here, $N_{C\min}$ equals to 2. Note that for small $M$, the empirical possibility is higher than the estimated distribution. It is attributed to many single path clusters being discarded. The mean number of clusters is 9.5 while the median is 10.

We investigate the property between cluster power and its mean excess delay shown in Fig. 6. In order to assemble different sets of channel parameters, all the power of clusters in one set is normalized. The cluster mean excess delay is the power-weighted average of the excess delays of all MPCs in the cluster. The least-squares (LS) criterion is applied to estimate the relationship between cluster power in dB and delay. An attenuation coefficient of $21.2dB/\mu s$ is found. Fig. 6 indicates that more clusters arrive in shorter mean delays. It is because MPCs have stronger powers if they are shorter delayed and they will be observed as long as their powers are within the dynamic range, thereby leading to an increased number of clusters.

Fig. 7 shows the dependence of cluster XPD on its mean excess delay. The XPD is defined as the ratio of the power of the copolarized component (VP-VP) to the power of the cross-polarized component (HP-VP), evaluated for each cluster. The linear regression has a slope of $15.9dB/\mu s$, hence, with increasing delay the VP-VP component gets stronger than

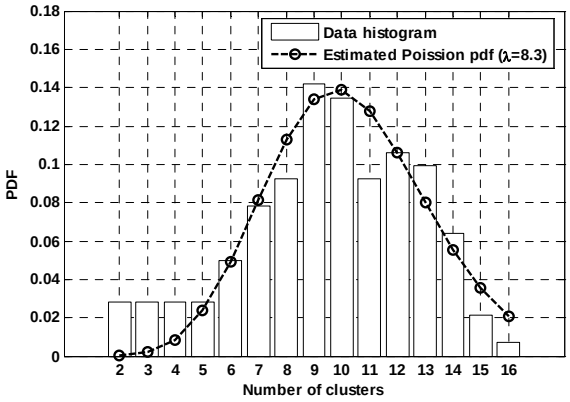


Fig. 5. Distribution of the number of clusters.

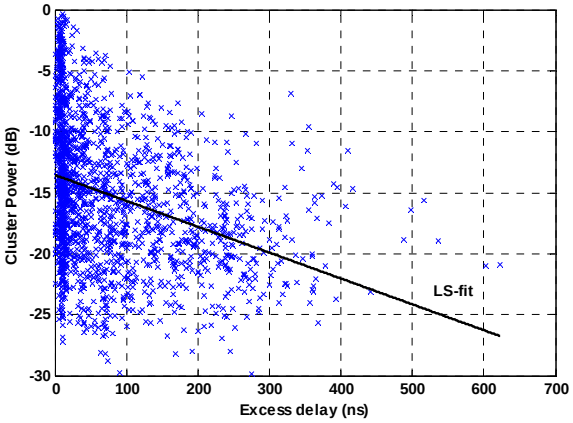


Fig. 6. Composite cluster power as a function of excess delay.

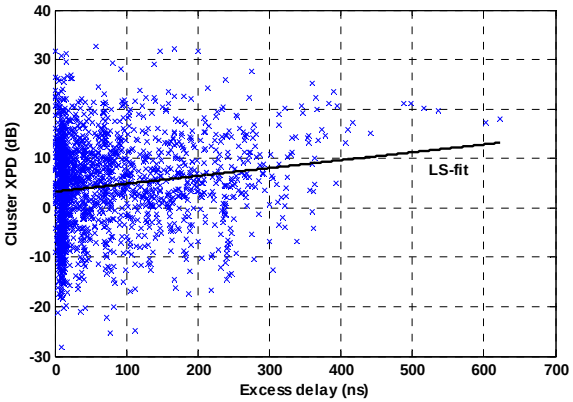


Fig. 7. Cluster XPD as a function of excess delay.

HP-VP component. Our result shows the same trend with that of [12] and [17]. However, the XPD is constant 8dB in microcellular environments in 3GPP model.

### *B. Intra-cluster Properties*

As shown in Fig. 8(a), the delay spread (DS) can be well modeled by the Lognormal distribution given by

$$f(x)=\begin{cases}\dfrac{1}{x\sigma\sqrt{2\pi}}\exp\left(\dfrac{-(\ln(x)-\mu)^2}{2\sigma^2}\right) & x>0\\ 0 & else\end{cases} \tag{9}$$

where $\mu$ and $\sigma$ are the mean and standard deviation, respectively. We find the mean value of 10.6 ns and median value of 4.3 ns of DS.

Fig. 8(b)-(d) show the cluster angular spreads for AOA azimuth, AOD azimuth, and AOD elevation with mean value $5.3^\circ$, $5.3^\circ$ and $4.3^\circ$, respectively. And also to avoid the ambiguity problem, we calculate the RMS AS $\sigma_{AS}$ as follows:

$$\sigma_{AS}=\sqrt{\frac{\sum_{i=1}^{L}(\varphi_{i,\mu})^2 P_i}{\sum_{i=1}^{L}P_i}}, \tag{10}$$

$\varphi_{i,\mu}$ is defined as

$$\varphi_{i,\mu}=\begin{cases}\varphi_i-\bar{\mu}_\varphi & |\varphi_i-\bar{\mu}_\varphi|\le\pi\\ 2\pi-|\varphi_i-\bar{\mu}_\varphi| & else\end{cases} \tag{11}$$

where $P_i$ and $\varphi_i$ is the power and AOA (or AOD) of the $i$th MPC in the cluster, respectively. $\bar{\mu}_\varphi$ is mean angle calculated as the method in (3)-(7). The Lognormal pdf fits to angular spreads with different mean and standard deviation values. Although AOD elevation spread has the smallest mean value among the three, it should not be neglected when terminals are rounded by rich scatterers in outdoor scenario.

## V. Conclusion

Cluster properties are characterized based on the outdoor wideband MIMO channel measurement campaign. The MPCs are found to arrive in clusters that are identified on azimuth of arrival-azimuth of departure-elevation of departure-delay domains. A method is developed to improve the automatic cluster identification algorithm in terms of convergence rate and accuracy, which can also be used in calculating AS to avoid the ambiguity caused by the origin of the coordinate system.

The clustering effect gives rise to two classes of channel parameters: inter-cluster and intra-cluster parameters. For the inter-cluster parameters, the number of clusters can be well modeled by Poisson distribution plus a minimum cluster number. The cluster powers decrease with increasing delay by about $21.2dB/\mu s$. We find that clusters with smaller delays have in general a higher XPD than that with larger delays with a coefficient of $15.9dB/\mu s$. For intra-cluster parameters, delay spread and angular spread all follow Lognormal distribution. It is suggested that the elevation angle should not be neglected when terminals are rounded by rich scatterers in outdoor scenario.

Although this work is mainly contributed to the hotspot application for IMT-Advanced system, the result can also be used in the peer-to-peer communication and cooperate systems.

## VI. Acknowledgment

The authors would like to thank the engineers of Elektrobit Company for their efforts in the measurement campaign. Useful discussions from J.-P. Nuutinen are greatly appreciated.

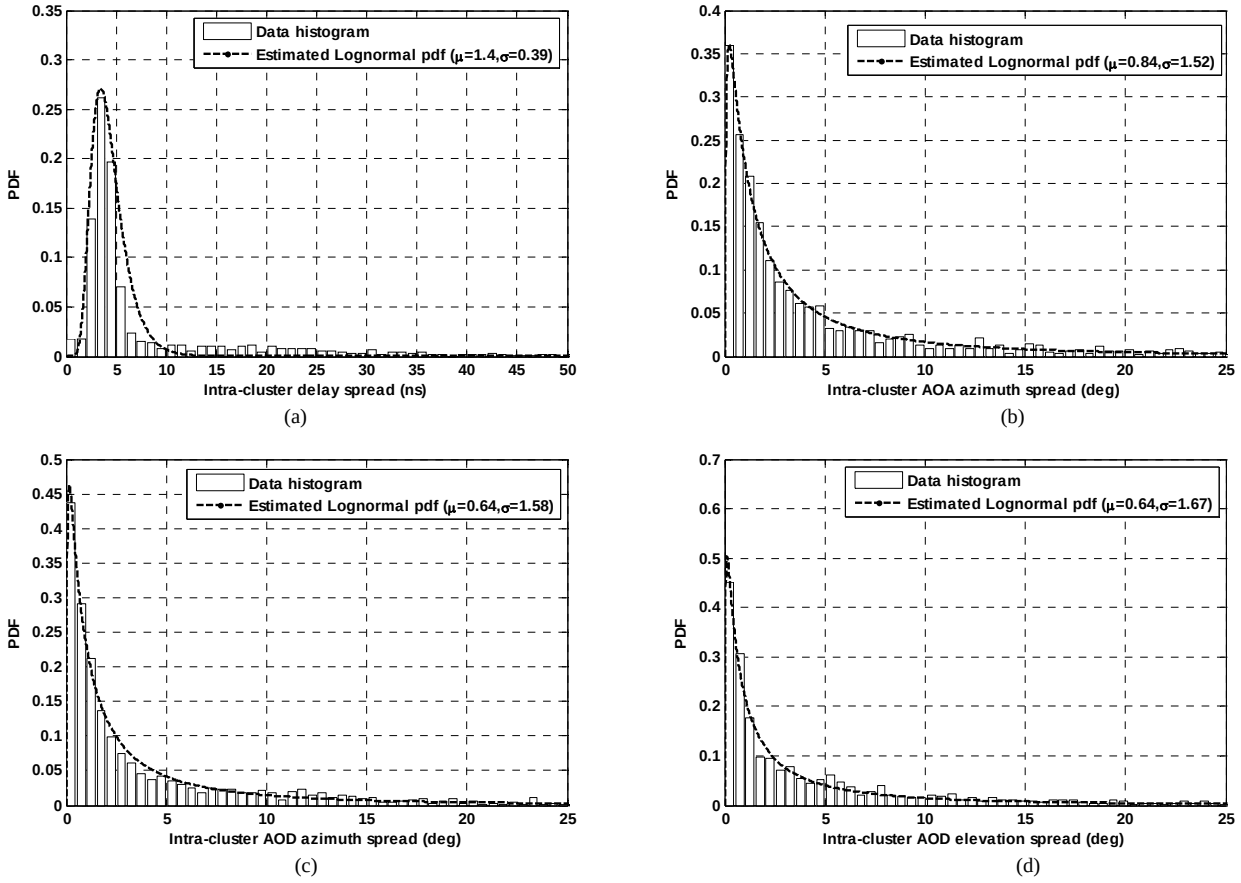


Fig. 8. PDFs of intra-cluster parameters. (a) Delay spread. (b) AOA azimuth spread. (c) AOD azimuth spread. (d) AOD elevation spread.

## REFERENCES


[1] ITU-R WP8F，Report IMT.NAME, "Naming for systems beyond IMT-2000," Oct. 2005.

[2] C.-C. Chong, C.-M. Tan, D. Laurenson, S. McLaughlin, M. Beach, and A. Nix, "A new statistical wideband spatio-temporal channel model for 5-GHz band WLAN systems," *IEEE Journal on Selected Areas in Communications*, vol. 21, no. 2, pp. 139 – 150, Feb. 2003.

[3] N. Czink, E. Bonek, L. Hentilä, J.-P. Nuutinen, J. Ylitalo, "Cluster-based MIMO channel model parameters extracted from indoor time-variant measurements," in *Proc. 49th Annual IEEE GLOBECOM Technical Conference & IEEE Communications EXPO*, San Francisco, CA, USA, November, 2006.

[4] L. Vuokko, P. Vainikainen, and Jun-ichi Takada, "Clusters extracted from measured propagation channels in macrocellular environments," *IEEE Trans. Antennas Propag.*, vol. 53, no. 12, Dec. 2005.

[5] K. Haneda, Jun-ichi Takada, and T. Kobayashi, "Cluster properties investigated from a series of ultrawideband double directional progation measurements in home environments," *IEEE Trans. Antennas Propag.*, vol. 54, no. 12, Dec. 2006.

[6] K.-H. Li, M. A. Ingram, and A. V. Nguyen, "Impact of clustering in statistical indoor propagation models on link capacity," *IEEE Trans. Commun.*, vol. 50, pp. 521-523, Apr. 2002.

[7] K. Yu, Q. Li, and M. Ho, "Measurement investigation of tap and cluster angular spreads at 5.2 GHz," *IEEE Trans. Antennas Propag.*, vol. 53, no. 7, pp. 2156-2160, Jul. 2005.

[8] N. Czink and P. Cera, "A novel framework for clustering parametric MIMO channel data including MPC powers," in COST 273 Post-project Meeting, Lisbon, portugal, Nov. 2005, available at http://www.nt.tuwien.ac.at/staff/nicolai-czink/.

[9] S. Wyne, N. Czink, J. Karedal, P. Almers, F. Tufvesson, and A. F. Molisch, "A cluster-based analysis of outdoor-to-indoor office MIMO measurements at 5.2 GHz," in *Proc. IEEE Vehicular Technology Conference 2006 Fall*.

[10] B. H. Fleury, "First- and second-order characterization of direction dispersion and space selectivity in the radio channel," *IEEE Transactions on Information Theory*, vol. 46, pp. 2027-2044, September 2000.

[11] Spatial Channel Model for Multiple Input Multiple Output (MIMO) Simulations (3GPP TR25.996), v6.1.0 (2003, Sept.). [Online]. Available: www.3gpp.org

[12] M. Shafi, M. Zhang, A. L. Moustakas, P. J. Smith, A. F. Molisch, F. Tufvesson, and S. H. Simon, "Polarized MIMO channels in 3-D: models, measurements and mutual information," *IEEE J. Sel. Commun*. vol. 24, NO. 3, March 2006.

[13] A. Stucki *et. al*., "PropSound System Specifications Document: Concept and Specifications," Elektrobit AG, Switzerland, Tech. Rep., 2001.

[14] B. H. Fleury, M. Tschudin, R. Heddergott, D. Dahlhaus, and K. I. Pedersen, "Channel parameter estimation in mobile radio environments using the SAGE algorithm," *IEEE J. Select. Areas Commun.*, vol. 17, pp. 438–450, Mar. 1999.

[15] M. Steinbauer, H. Özcelik, H. Hofstetter, C. F. Mecklenbräuker, and E. Bonek, "How to quantify multipath separation," *IEICE Trans. Electron.*, vol. 85, pp. 552-557, Mar. 2002.

[16] L. Correia, ed., COST 273 final report: Towards mobile broadband multimedia networks. Elsevier, 2006.

[17] M. Toeltsch, J. Laurila, K. Kalliola, A. F. Molisch, P. Vainikainen, and E. Bonek, "Statistical characterization of urban spatial radio channels," *IEEE J. Sel. Commun.* nol. 20, NO. 3, Apr. 2002.